Journal of Thermal Analysis and Calorimetry (2023) 148:6047–6057
https://doi.org/10.1007/s10973-023-12152-x

Use of MTDSC in the detection of weak glass transitions: the hysteresis peak

Joseph D. Menczel[1] · Aditya Jindal[2] · Michael P. Mallamaci[2] · Tonson Abraham[3]

Received: 18 July 2022 / Accepted: 24 March 2023 / Published online: 13 April 2023

Abstract
Miscibility of poly(butylene terephthalate, PBT) with a PVC plasticizer (PN-250) has been characterized by modulated temperature DSC measurements. The glass transition parameters were measured by total heat flow measurements as the midpoint of the heat capacity increase (for the PBT rich areas) and by creating an endothermic hysteresis peak at the glass transition of the plasticizer, because there was no low temperature baseline due to the low T_g of PN-250. The disadvantage of this method is that it does not allow determination of the heat capacity jump at the glass transition. Partial miscibility was determined between these two components. It was observed that crystallinity of PBT in the blends was much higher than in neat PBT because of the higher segmental mobility of the polymer segments in the blends. The hysteresis peak at the PBT glass transition in the blends is much narrower and more intense than for neat PBT since the mobile amorphous fraction of PBT is higher in the blends. Together with the lower rigid amorphous fraction, this means sharper boundary between the mobile amorphous fraction and the PBT crystallites.

Keywords Modulated temperature DSC (MTDSC) · Glass transition · Hysteresis peak at the glass transigtion · Poly(butylene terephthalate)(PBT) · Plasticizers · Heat capacity increase at the glass transition

Introduction

Commercially available TPVs (thermoplastic vulcanizates) with the highest performance (good elastic recovery at the 90 °C to 100 °C maximum continuous use temperature) are produced by dynamic vulcanization of ethylene-propylene-diene (EPDM) rubber in isotactic polypropylene (PP). In these cases it is necessary to add substantial quantities of paraffinic oil to the formulation for product processability to achieve optimum molten product melt viscosity and temperature control during TPV reactive extrusion. This also helps to improve the product appearance [1]. In the dynamic vulcanization process, high molecular mass (MM) PP is melt-blended with high MM EPDM, under intense shearing conditions provided by a corotating twin screw (TSE) extruder. In the dynamic vulcanization process additional oil may be added to the intimately melt-mixed PP/EPDM blend, kept at about 200 °C. Thus, a two-phase system, consisting of an oil-swollen EPDM rubber phase and a solution of PP in oil is produced. Subsequently, a curative that selectively cures the rubber phase without affecting the plastic phase, is injected into the two-phase system, while intensive melt mixing is continued. The action of the curative causes the rubber phase to break up into oil-swollen cross-linked particles that are contained in a solution of PP in oil. The volume of the solution of PP in oil is generally smaller than the volume of the oil-swollen EPDM phase, but it must be large enough to be continuous after dynamic vulcanization. On cooling, PP crystallizes from the oil solution, and the oil rejected from the PP crystalline phase further swells the particulate rubber, while a portion of this oil is included in the PP amorphous regions. The morphology of the final room temperature product consists of oil-swollen, cross-linked rubber particles of 1to 5 μm diameter, and these are contained in a continuous, oil-swollen, semi-crystalline PP matrix [2].

The health, environmental, and economic benefits of PP/EPDM thermoplastic vulcanizates (TPVs) resulted in the

This paper has been presented at the 2022 48th Annual NATAS Conference, August 1–5, 2022, Cleveland, OH.

✉ Joseph D. Menczel
jmenczel@yahoo.com

[1] Thermal Measurements, 412 Stampede Court, Fort Worth, TX 76131, USA

[2] Parker Hannifin Corporation, Fluid Connectors Group, 6035 Parkland Boulevard, Cleveland, OH 44124, USA

[3] Tonson Abraham Consulting, LLC, 39467 Clayton Drive, Avon, OH 44011, USA

replacement of thermoset hydrocarbon rubbers in many applications. However, the replacement of high-temperature (150 °C continuous use temperature), hydrocarbon-oil resistant thermoset elastomers with TPVs had limited success only.

High temperature, oil-resistant TPVs can also be produced by the dynamic vulcanization of polar rubbers. Semicrystalline polymers are preferred for TPV preparation [3]. In this connection, Nylon 6 and PBT are the most suitable semicrystalline candidate materials. The amount of plastic phase of the TPV is the only suitable method to control TPV hardness, unlike fillers like carbon black that are routinely used to control the hardness of a thermoset rubber [4]. The required amount of plastic phase in a TPV formulation is limited by the need for soft products (Shore A hardness 70–90) in many applications. Low amounts of the plastic phase can disallow its continuity, which, as mentioned above, would be detrimental to TPV processability and physical properties. Hence, it is necessary to add a plasticizer to the TPV formulation that is preferably melt miscible with the TPV plastic phase over that with the TPV rubber phase, and that is also substantially present in the amorphous component of the semicrystalline plastic on crystallization of the TPV melt blend. The relatively high glass transition temperature (T_g) of Nylon 6 (~60–70 °C) and PBT (40–50 °C), compared with the lower T_g of high temperature, oil-resistant rubbers such as ACM polyacrylate rubbers [5], can be detrimental to TPV low temperature mechanical properties such as impact strength but the lower use temperature properties of the TPV may be improved by adding a low T_g plasticizer to the system that is miscible with the amorphous phase of the semicrystalline polymer, It may also be sufficient if the plasticizer is contained in the system as an immiscible fine dispersion. For example, the notched Izod impact of PP at 0 °C is improved by the presence of a low mass fraction (7%) of dioctyl sebacate [6].

In such cases, the low temperature notched Izod impact improvement of PP/EPDM TPVs containing polar plasticizers instead of hydrocarbon plasticizers is credited to increased reduction of T_g of both the plastic and rubber phase [6]. Notched Izod impact strength increase is also observed for amorphous polymers such as polystyrene containing a fine dispersion of a low T_g immiscible component like polybutadiene [7, 8] (Fig. 1).

In connection with the preparation of high-temperature, oil-resistant thermoplastic vulcanizates (TPVs), it is of interest to identify plasticizers that are melt miscible with polar, semicrystalline plastic materials such as poly (butylene terephthalate) (PBT), where the melting point varies between 220° and 230 °C [9]. We remind the reader that one such plasticizer is quite common in a certain type of polymers: this is water absorbed by various Nylons. In everyday life water is everywhere, and it is virtually impossible to isolate Nylon products from water being present as moisture in the atmosphere. Various Nylon products may contain as much as 8%, water and taking into account that the crystallinity of semicrystalline Nylons is around 50%, the local water concentration may be as high as 15%.

Since the Hansen solubility parameters of PVC and PBT are close to each other [($\delta = 21.3$ (MPa)$^{1/2}$ [10] and $\delta = 23.1$ (Mpa)$^{1/2}$) [11], respectively] we opted to evaluate a commercially available, low T_g PVC plasticizer, namely PN-250 ($T_g = -65$ °C), as a PBT plasticizer. The Hansen solubility parameter developed by Hansen [12, 13] can be predicted if some material dissolves in another and forms a solution. In the theory of Hansen every material is given three Hansen parameters characterizing the

- energy from dispersion forces between molecules;
- energy from dipolar intermolecular force between molecules, and
- energy from hydrogen bonds between molecules or molecular segments.

These three parameters are usually treated as co-ordinates for a point in a three dimensional space known as the Hansen space. The closer the two molecules are in the Hansen space, the more likely they will dissolve in each other. In addition, the Hansen sphere radius (R_0) is used to characterize the substance being dissolved. If R_0 is the radius of the sphere, its center is determined by the three Hansen parameters. To calculate the distance (R_a) between Hansen parameters in the Hansen space, the following formula is used:

$$\left(\mathrm{R_a}\right)^2 = 4\left(\delta_{d2} - \delta_{d1}\right)^2 + \left(\delta_{p2} - \delta_{p1}\right)^2 + \left(\delta_{h2} - \delta_{h1}\right)^2 \quad (1)$$

When this equation is combined with R_0, we obtain the relative energy difference for the system:

$$\Delta E = \mathrm{R_a}/R_0 \quad (2)$$

When $\Delta E < 1$, the two types of molecules are similar and dissolution will take place. When ΔE is around 1, partial dissolution will take place, and at $\Delta E > 1$, no dissolution occurs.

On the basis of the solubility parameters, some miscibility is expected between PBT and PN-250.

Miscibility of two polymers (or a polymer and a low molecular mass substance) can be determined by the glass

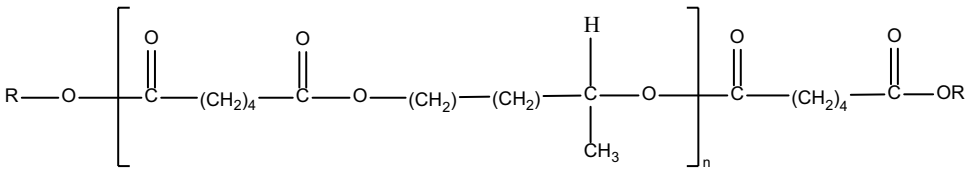

Fig. 1 The molecular structure of ADK Cizer PN-250 from Adeka Corporation (Japan)

transition temperatures. When the two polymers are not miscible, the blend will display the two glass transitions at the same temperature as the constituting polymers. In case of partial miscibility the glass transitions are still separate, but they are shifted toward each other. Finally, when the two polymers are miscible, the sample will display one glass transition, and the T_g that can be calculated either by the Fox or the Gordon-Taylor equation or one of the Couchman-equations depending on the composition [14, 15, 17].

In thermal analysis of polymers quite often it is difficult to determine the glass transition temperatures by DSC. In this method, the glass transition is displayed as a jump in the heat capacity. However, due to a number of reasons the glass transition can be broadened. Such shallow glass transitions can be seen for semicrystalline polymers, highly oriented samples (oriented films or fibers) or for samples containing particles of very small sizes. In such cases, it is difficult to see the glass transition, but the phenomenon of enthalpy relaxation can be used to improve its visibility. Two sources can be used to introduce an enthalpy relaxation (hysteresis peak):

(a) When a sample is cooled slowly and reheated fast, an endothermic peak is overlaid on the high temperature side of the glass transition measured in the heating run, or
(b) The sample can be annealed 10–20 °C below the expected glass transition temperature. In this case a similar hysteresis peak can be seen as the one described in (a).

Of course, the endothermic hysteresis peak is much better visible than a shallow shift in the baseline given by the heat flow vs. temperature curve. However, as found by Menczel and Wunderlich [21], the hysteresis peak will not appear in the traditional DSC curves of semicrystalline polymers when the sample is cooled at a lower rate and reheated at a higher rate (case "a"). But even for semicrystalline polymers the hysteresis peak can be introduced in the traditional DSC curves by annealing (case "b"). In case of amorphous polymers the hysteresis peak is the consequence of the time dependence of the glass transition. When the sample is being cooled slowly (curve 1 in Fig. 2) and reheated fast (curve 2 in Fig. 2), the glass transition on heating will be shifted to higher temperatures, because the ramp rate is higher on heating than on cooling. However,

$$\int_0^T C_p \mathrm{d}T = H_T \tag{3}$$

This means that the area under the DSC curve is the absolute enthalpy. According to equilibrium thermodynamics, the enthalpy must have a definite value, i.e., the area under the DSC curve must have a definite value and this may depend on the condition of the sample only, and cannot depend on how we got to this point. But then for the heated sample a smaller enthalpy would be obtained than for the cooled sample, and this is not allowed by thermodynamics. So, we must get back some correction of the DSC curve on heating, because we would lose area B. Thus, an endothermic hysteresis peak will be overlaid on the heating curve, and the area under the hysteresis peak (A) will be exactly the same as area B [16].

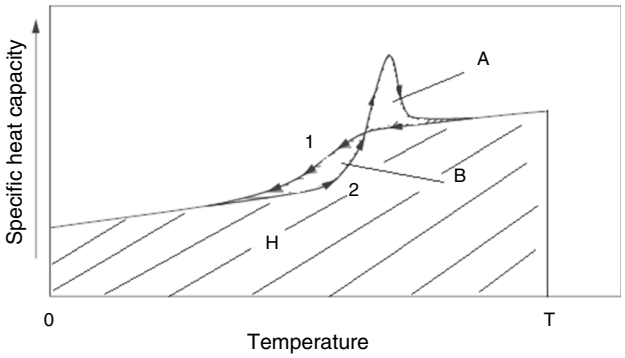

Fig. 2 The source of the hysteresis peak [slow cooling (1), fast reheating (2)]: the sample is cooled from T to 0 at a rate CR, and reheated from 0 to T at a rate HR (HR > CR). According to equilibrium thermodynamics A = B, that is the area under the two curves must be equal [16]

This is the phenomenon that can be used to make the glass transition visible: we must cool the sample slowly and reheat it fast, and we will get an endothermic peak on the higher temperature side of the glass transition. The greater the difference between the cooling and heating rates, the more intense the magnitude of the hysteresis peak. That is, if we cool the sample at a rate of 2 °C min^{-1} and reheat it at a rate of 10 °C min^{-1} (case 1), and in another case cool the sample at a rate of 5 °C min^{-1} and reheat it at 10 °C min^{-1} (case 2), the hysteresis peak in case 1 will be more intense than in case 2. This phenomenon can even be further magnified if we separate the hysteresis peak from the heat capacity jump of the glass transition. This can be done using modulated temperature DSC (MTDSC): the non-reversing signal will show the kinetic effects (the hysteresis peak), and the reversing signal will show the thermodynamic effects (the heat capacity jump). In this paper, these methods were used to detect the glass transitions of the samples.

Experimental

The DSC curves were recorded on a TA Instruments Q2000 DSC cooled by an RCS 90 cooling unit. In most cases the samples were cooled at 2 °C min^{-1} and reheated

at 5 or 10 °C min^{-1} in modulated mode (when the Q-series DSCs or Discovery DSCs are used in MT-DSC measurements, the underlying heating rate can be as high as 10 °C min^{-1} if the sample mass is limited to about 5 mg). As will be seen in the paper, the reason for the choice of the cooling and heating rates was the intention to create a hysteresis peak at the glass transition of PN-250. For this cooling rates slower than the subsequent heating rates are required. Since the heating rates in this work were 5 or 10 °C min^{-1}, 2 °C min^{-1} cooling rates were used. During the cooling experiments, there was no straight low temperature baseline on the cooling trace, because in most cases the temperature control was lost at ca. − 70 °C (the instrument is unable to cool at a linear rate of 2 °C min^{-1} at temperatures lower than − 70 °C). The samples then were equilibrated at − 90 °C, and reheated at a rate of 5 or 10 °C min^{-1}. When DSC heating starts from isothermal conditions, the heat flow signal suddenly shifts into the endothermic direction, and the magnitude of this shift is proportional to the heat capacity of the sample (this is the phenomenon used to measure specific heat capacity by DSC) and the heating rate. The temperature range necessary to accomplish this shift is instrument dependent. In power compensation DSC's (Perkin-Elmer), this shift is around 15–20 °C wide, while it is somewhat broader in heat flux DSC's (like TA Instruments DSCs). It also depends on the starting temperature of the run and the heating rate. In the case of PN-250 (starting temperature of the run is − 90 °C) the shift takes place between − 90 °C and ca. − 60 °C. The *y*-axis magnitude of this shift is considerably bigger than the height of the heat capacity jump due to the glass transition, so no linear low temperature baseline can be seen, the baseline is "swallowed" by the isothermal → ramp shift. Thus, in this case, the heating can be modulated and the curve can be separated into the hysteresis peak in the non-reversing heat flow and the heat capacity jump in the reversing heat flow and the hysteresis peak can be used as the indication of the glass transition. This separation is even more important for the blend samples as will be seen below. Since this problem with the start of the heating runs was seen for all samples, all heatings were done in modulated mode, and the glass transition temperature was determined as the peak temperature in the non-reversing signal. Sometimes the glass transition temperature was determined in the traditional way, i.e., by the midpoint of the heat capacity jump. The two described methods should not give glass transition temperatures differing more than around 5 °C. As will be seen below, the measured values of the glass transition temperature by the two described methods will not differ more than 4–5 °C. This method gave a glass transition temperature between − 67.0 °C and − 60.0 °C using the hysteresis peak. For samples with high PN-250 content the glass transition could also be measured approximately as the midpoint of the heat capacity increase flow curve gives T_g as − 65.0 °C. The heat capacity jump at the glass transition is ca. 0.340 Jg^{-1} $°C^{-1}$ (the large scattering of the peak temperature of the hysteresis peak is due noises and not perfect linear cooling rate at very low temperatures). The results are summarized in Table 1.

In the present work, Valox 315® PBT (from SABIC) was blended with ADK Cizer PN-250 (Fig. 1). Plaques were prepared of PBT and the blend samples by compression molding and extrusion as described below.

The structural assessment of PN-250 is based on comparison of proton magnetic resonance spectra (PMR) of this material with the published PMR spectrum of poly (1,3-butylene adipate) [23]. Our findings concerning the solid-state phase morphology of melt blends of PBT and PN-250, as inferred by DSC, is reported in this paper.

The blend samples were prepared by two different methods:

Table 1 Crystallization and melting parameters of Valox 315 PBT plaques

Sample	Cooling		2nd heating						
			Glass transition			Melting			
	T_{co}	T_{cp}	T_g	ΔC_p	MAF	T_{mp}	T_m	ΔH_f	RAF
Compr.m.#1	203.5	195.5	44.0	0.081	23	222.0	235.0	33.2	53
Compr.m.#2	203.0	195.0	41.0	0.088	25	222.0	234.5	34.7	50
c.m.average	203.5 ± 0.5	195.5 ± 0.5	43.5 ± 0.5	0.085 ± 0.005	24	222.0	235.0 ± 0.5	34.4	51
Twin screw #1	202.0	192.5	43.0	0.124	35	224.0	233.5	43.8	34
Twin screw #2	201.0	192.5	42.5	0.123	35	223.5	233.0	45.0	33
Twin screw #3	201.0	192.5	41.0	0.120	34	224.0	234.5	42.4	36
Twin screw averages	201.5 ± 0.5	192.5	42.0 ± 1.0	0.122 ± 0.002	35	224.0 ± 0.5	233.5 ± 1.5	43.7 ± 1.3	34

The dimensions of the parameters in Table 1 are the following: T_{co}, T_{cp}, T_g, T_{mp}, T_m is °C; ΔC_p is Jg^{-1} g^{-1}; ΔH_f is Jg^{-1}; MAF and RAF %

Compression Molding

Two samples were compression molded in this work: PBT and PBT-PN-250 blends.

PBT and PN-250 were melt mixed in a laboratory mixer at about 250 °C for 5 min at a shear rate of about 100 s^{-1}, and subsequently compression molded, but PBT was only compression molded. The mentioned significant increase of the PBT crystallinity in the blends suggest that PBT could be partially or completely dissolved in PN-250 during melt mixing, so the chain disentanglement of PBT would contribute to the increase of PBT crystallinity in the blends. Similar phenomena have been reported by other authors for PBT [23].

Twin screw compounding

A PBT/PN250 melt blend (80 mass% PBT + 20 mass% PN250) was also compounded on a ZSK 26 mm, 10-barrel, co-rotating, Coperion two-lobe twin-screw extruder with L/D = 40:1. The maximum torque per screw shaft for this extruder is 106 Nm, the maximum allowable horsepower is 36 HP, and the maximum allowable screw speed is 1200 RPM. PBT was fed into the feed throat, and PN250 was fed into barrel #3 using a liquid injector. Barrels #4 and #9 were vented to the atmosphere. The total feed rate was 30 lb hr^{-1}, and the screw speed was 150 RPM. The barrels were set at a temperature of 260 °C with the die set at 270 °C. The screw design had a combination of conveying and low-intense kneading elements to effectively melt the plastic and prepare the melt blend of PBT and PN250. After extrusion, the strands were water-cooled, pelletized, and dried for molding the test samples.

Injection Molding

A Sumitomo Systec 90–310 injection molding machine with three heated zones (barrel set temperatures: 235 °C, 240 °C, and 245 °C, with the nozzle set at 250 °C) was used for injection molding. The screw speed was 150 rpm, and the injection pressure was between 11–18 Mpa.

Results and discussion

PBT

Valox 315 PBT was used in these series of measurements. The PBT plaque was prepared in similar way as the PBT/PN-250 blend plaques, i.e. it was compression molded. The samples were heated from about − 50 °C to 275 °C at a rate of 10 °C min^{-1}, then cooled at 10 °C min^{-1} (cooling) and finally reheated at 10 °C min^{-1} (2nd heating). For characterization and comparison with the blend samples, the cooling and 2nd heating data were used, because the 2nd heating samples had definite thermal history. The results are summarized in Table 1. In this table, T_{co} is the starting temperature of crystallization, T_{cp} is the peak temperature of crystallization, T_g is the glass transition temperature (the temperature of half heat capacity increase at the glass transition), ΔC_p is the heat capacity increase at the glass transition, T_{mp} is the peak temperature of melting, T_m is the melting point (the temperature of the last, highest temperature of the melting endotherm), and ΔH_f is the heat of fusion. From the ΔC_p and ΔH_f, the mobile amorphous fraction (MAF) and the rigid amorphous fraction (RAF) can also be calculated. For this we need the heat capacity jump at the glass transition of amorphous PBT that was determined by Cheng et al. [19] as 77 J $°C^{-1}$ mol^{-1}. This value seems reasonable for ΔC_p of the 100% amorphous PBT estimated by Wunderlich's rule [20]. This rule says that the heat capacity increase of the totally amorphous polymer can be approximated if we take 11.3 J g^{-1} $°C^{-1}$ for every bead (mobile unit) in the repeating unit, and sometimes double or triple this value for the large chemical groups, like the phenylene group.

Wunderlich's rule gives then a value of ΔC_p between 79 and 90 J$°C^{-1}$ mol^{-1} for PBT which is not very far from the 77 J$°C^{-1}$ mol^{-1} determined by Cheng et al. [19]. The crystallinity can be estimated by accepting 140 Jg^{-1} for $\Delta H_f°$ (the equilibrium heat of fusion [24]). Then the rigid amorphous fraction can be calculated by the following equation:

$$\mathrm{RAF} = 100 - (\alpha + \mathrm{MAF}) \tag{4}$$

Here, RAF is the rigid amorphous fraction, %; α is the crystallinity, %; and MAF is the mobile or traditional amorphous fraction, &. The crystallization and melting curves of Valox 315 PBT are shown in Figs. 3 and 4, the thermal parameters are summarized in Table 1. The measurements were carried out in modulated mode with ± 0.5 °C/40 s modulation parameters. As will be shown below, the glass transition of PN-250 in the blend samples had to be measured in modulated mode, since the low temperature T_g values were too close to the starting temperature of the runs.

In addition to the compression molded samples, several extruded samples were measured. As can be seen in Table 1, the glass transition temperature, the peak temperature of melting and the melting point of PBT are not sensitive to the processing method, but the crystallization temperature, the heat capacity jump at the glass transition and the crystallinity (therefore, also the mobile amorphous fraction and the rigid amorphous fraction) are considerably different for the compression molded and extruded

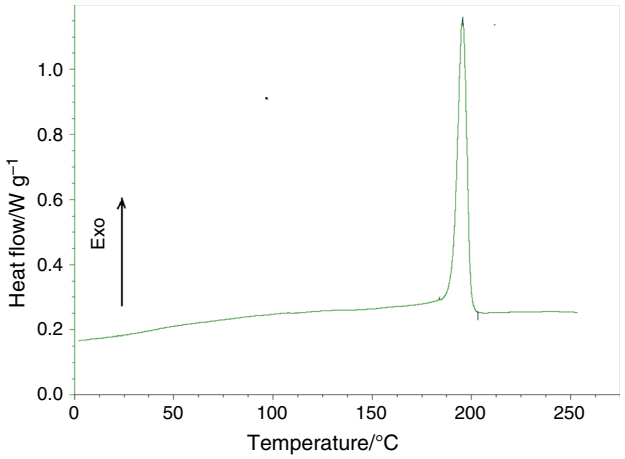

Fig. 3 The crystallization curve of Valox 315 PBT at 10 °C min^{-1}

PBT samples. Therefore, in the later calculations the data obtained for the compression molded samples were used for comparison with the blend samples. The glass transition, melting and crystallization parameters for the two PBT plaques (compression molded and extruded) are summarized in Table 1. The glass transition temperature and the melting parameters seem not to have been influenced by the processing, but the other parameters do depend on the type of processing. In addition to the compression molded samples, several extruded samples were measured. As can be seen in Table 1, the glass transition temperature, the peak temperature of melting and the melting point of PBT are not sensitive to the processing method, but the crystallization temperature, the heat capacity jump at the glass transition and the crystallinity (therefore, also the mobile amorphous fraction and the rigid amorphous fraction) are considerably different for the compression molded and extruded PBT samples. We can only guess about the reason of this phenomenon, but cannot find the reason for it. In the later calculations the data obtained for the compression molded samples were used for comparison with the blend samples.

- The peak temperature of crystallization of the extruded PBT is somewhat lower than for the compression molded samples;
- The mobile amorphous fraction (MAF) for the compression molded samples is much lower than for the extruded samples, while the crystallinity is also lower. As a consequence, the rigid amorphous fraction in the compression molded samples is much higher than in the extruded samples.
- Obviously, to record the glass transition of PBT is simple, although the transition is broad and shallow due to the crystallinity. When the rigid amorphous phase was found by Menczel and Wunderlich [21], it was reported that the hysteresis peak is missing at the glass transition of semi-crystalline polymers. Later Menczel did find the hysteresis peak in MTDSC recordings [25], although the intensity of the hysteresis peak is small (Figs. 5–7). Thus, as can be seen in a number of figures in this publication, the hysteresis peak of PBT can be clearly seen in the blend samples as well (see e.g., Figs. 8–10). It is noteworthy that in the DSC curves of the blends the hysteresis peak of PBT is narrower and more intense than in neat PBT, and this probably indicates higher mobility in the mobile amorphous phase of PBT in then blends than in PBT.

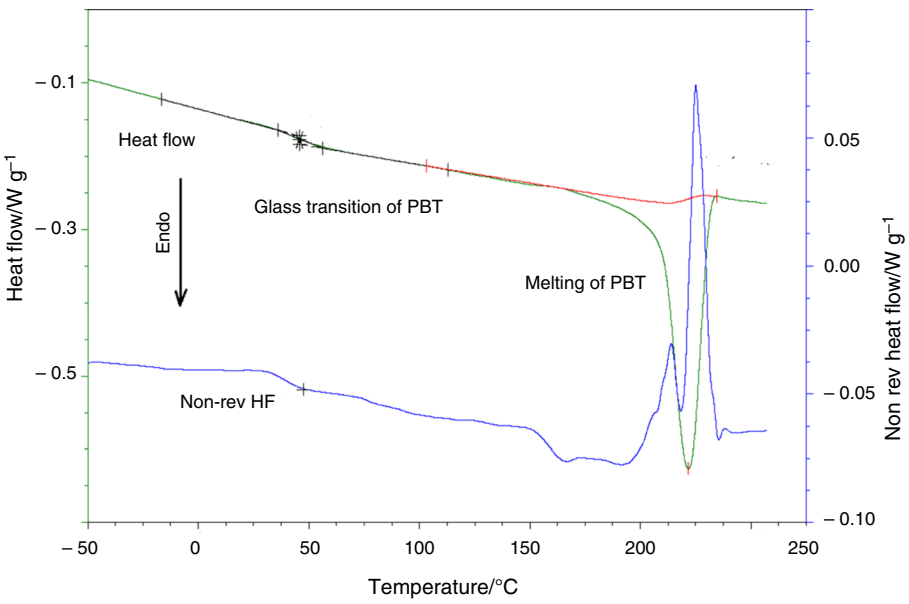

Fig. 4 The melting curve of Valox 315 PBT recorded in MTDSC mode (the total heat flow and non-reversing heat flow curves). First heating from − 50 to 265 °C, UHR = 10 °C min^{-1}

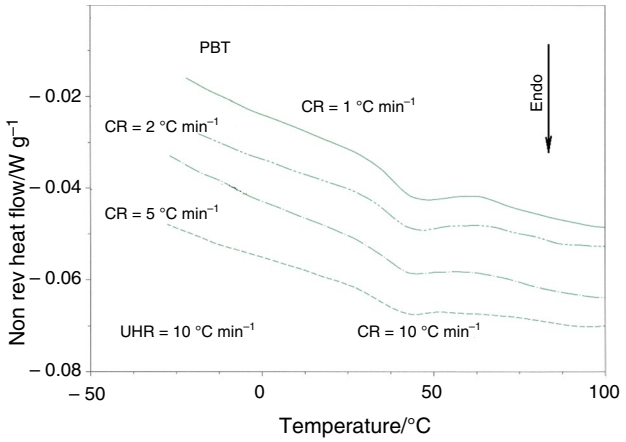

Fig. 5 The hysteresis peak on the non-reversing signal at the glass transition of poly(butylene terephthalate) after cooling at 1, 2, 5 and 10 °C min^{-1}. Underlying heating rate 10 °C min^{-1}, modulation ± 0.5 °C/40 s. The intensity of hysteresis peak increases with decreasing cooling rate. There is a weak endothermic peak on the curve of the sample cooled at 10 °C min^{-1} because the sample is being annealed during the heating

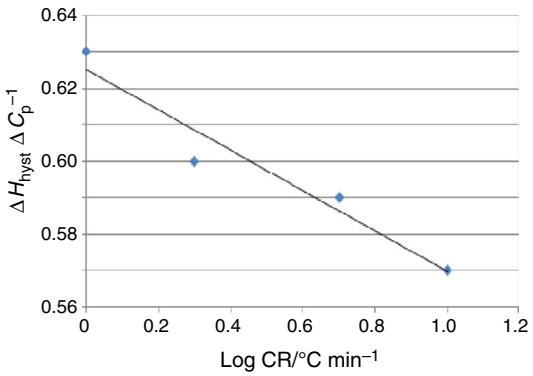

Fig. 6 The relative intensity of the hysteresis peak at the glass transition of PBT as a function of logarithm cooling rate

PN-250

These samples were cooled at a rate of 2 °C min^{-1} and reheated at 5 °C min^{-1}. In other experiments 2 °C min^{-1} to 5 °C min^{-1} and 5 °C min^{-1} to 10 °C min^{-1} cooling-heating rate combinations were used. The glass transition temperature of PN-250 on cooling is −65.0 or −66.0 °C at both 2 and 5 °C min^{-1} cooling. Unfortunately, there is no straight low temperature baseline on the cooling curves, because the temperature control is lost at ca. −70 °C (the instrument is unable to cool at a linear rate at temperatures lower than −70 °C). The sample then was equilibrated at −90 °C, and heated at a rate of 5 °C min^{-1}. When any DSC heating

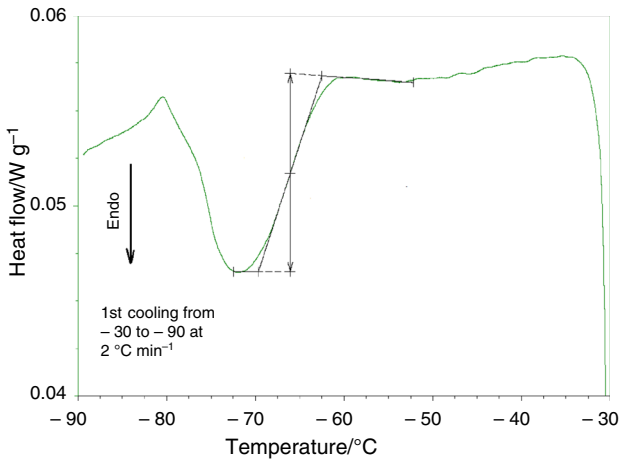

Fig. 7 The DSC cooling curve of PN-250 recorded at a rate of cooling of 2 °C min^{-1}

starts from isothermal conditions, the heat flow signal suddenly shifts due to the isothermal → ramp mode change, and the magnitude of this shift is proportional to the heat capacity of the sample (this is the phenomenon used to measure specific heat capacity by DSC). The width of this shift to reach steady state depends on the instrument (the time constant), the starting temperature of the run, the heating rate and the environmental temperature. In the case of PN-250 (starting temperature of the run is −90 °C) the shift takes place between −90 °C and ca. −60 °C. The *y*-axis magnitude of this shift is considerably larger than the heat capacity jump at the glass transition, because the absolute value of the heat capacity of a polymer is much higher than the heat capacity jump at the glass transition. Therefore, if the starting temperature of the run is close to the transition, no linear low temperature baseline can be seen, the baseline is "swallowed" by the isothermal → ramp shift. So, in this case, the heating run can be modulated and if the previous cooling rate is smaller than the following heating rate, a hysteresis peak will be overlaid on the curve at the higher portion of the glass transition. In the present measurements the modulation was ± 0.5 °C/40 s, thus the hysteresis peak can be separated out into the non-reversing heat flow. As will be shown below, this separation is even more important for the blend samples. Since this problem with the start of the runs was present for all samples, all heatings were done in modulated mode, and the glass transition temperature could be determined as the maximum temperature of the hysteresis peak in the non-reversing signal (and the midpoint of the heat capacity increase if that signal could be seen because of frequent sensitivity problems). This method gave a glass transition temperature between −67.0 °C and −60.0 °C, while the midpoint of the heat flow curve was T_g as −65.0 °C. Average heat capacity jump at the glass transition was ca. 0.340 Jg^{-1} °C^{-1}. The results are summarized in Table 2.

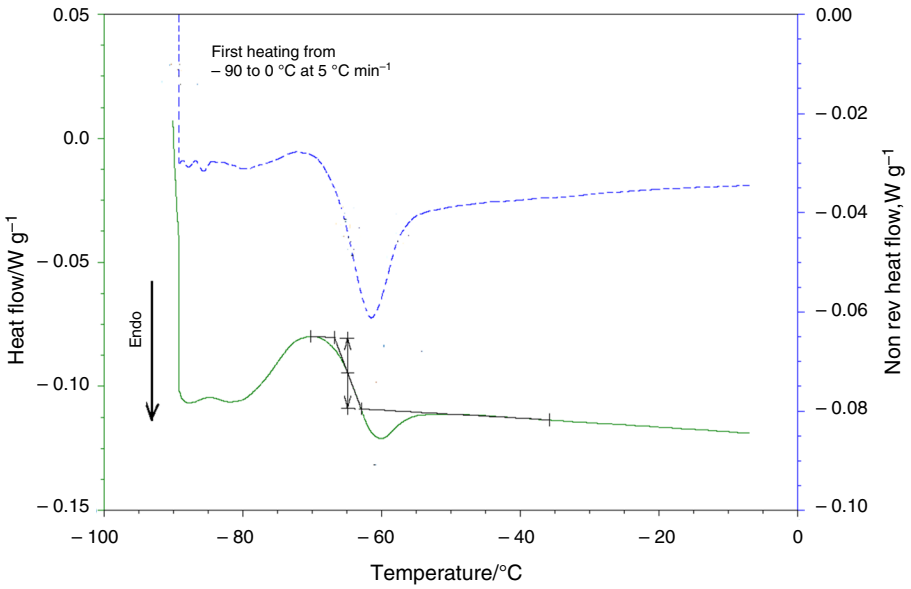

Fig. 8 The DSC heating curve of PN-250 recorded in MTDSC mode. The underlying heating rate is 5 °C min^{-1}. Solid line: Heat Flow; dashed line: NonReversing Heat Flow. As can be seen the low temperature baseline (the baseline below the glass transition) is missing, therefore the ΔC_p is approximate only

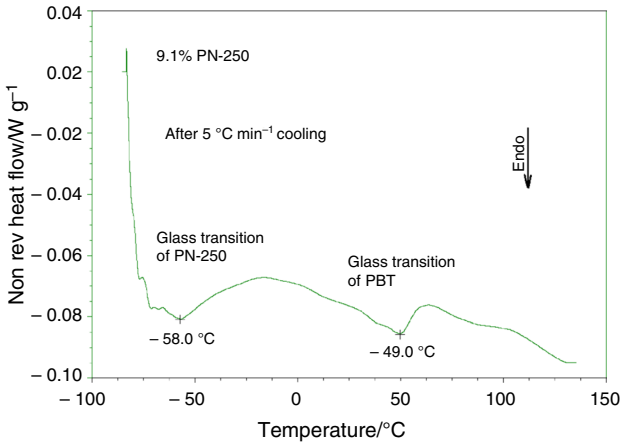

Fig. 9 The non-reversing heat flow as a function of temperature for a PBT/PN-250 blend with 9.1% of the plasticizer. The T_g of the PN-250-rich phase is −58.0 °C, while the T_g of the PBT-rich phase is 49.0 °C

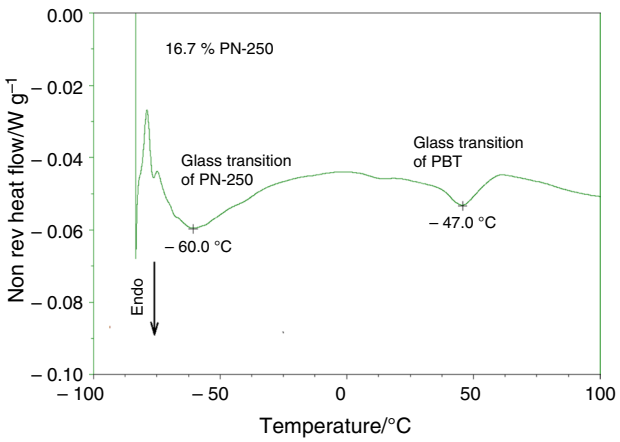

Fig. 10 The non-reversing heat flow as a function of temperature for a PBT/PN-250 blend with 16.7% of the plasticizer. The T_g of PN-250 is −57.0 °C, while the T_g of the PBT is 49.5 °C

PBT/PN-250 blend samples

Blend samples with three different PN-250 contents were run. These were 9.1, 16.7 and 28.5 mass % PN-250 containing compression molded samples. In addition, for clarifying the effect of the processing method on the structure of the blends, an extruded sample containing 20% PN-250 was also prepared Tables 3 and 4).

For these samples, it is much more difficult to record the PN-250 glass transition than for pure PN-250, because in addition to the low temperature baseline problem (there is no linear low temperature baseline due to the isothermal→ramp signal change), there is a sensitivity problem, so it is not easy to recognize the heat capacity jump at the glass transition. Therefore, as mentioned above, we tried to introduce a hysteresis peak with slow cooling (2 °C min^{-1}) followed by faster heating (5 or 10 °C min^{-1}) in modulated mode. The modulation parameters as for pure PN-250 were ±0.5 °C/40 s. The hysteresis peak was separated out into the non-reversing heat flow as shown in Figs. 8–10. The calculated phase structure (mobile amorphous fraction, rigid amorphous fraction and crystallinity are detailed in Table 4.

The calculated data indicate that the transition temperature of the lower glass transition (measured as the peak temperature of the hysteresis peak) decreases with

Table 2 Measurement of the glass transition temperature of PN-250

T_g on cooling°C/cooling rate/°C min^{-1}	T_g (from heat flow) on Heating/°C/heating rate/°C min^{-1}	T_g (hysteresis peak temp)/°C/heating rate/cooling rate/°C min^{-1}
−66.0/2	−65.0/5	−67.0/5/2
−65.5/2	−65.0/5	−62.5/5/2
−65.5/2	−65.0/5	−62.5/5/2
−66.0/2	−65.5/10	−60.0/10/2
−65.0/2	−65.0/10	−65.0/5/2
Averages: −65.5	−65.0 ± 0.2	−63.5 ± 2.5

Table 3 Thermal Properties of the PBT/N-250 Blends

Sample	Cooling		2nd heating					
	T_{co}	T_{cp}	T_{g1}	T_{g2}	ΔC_p (for T_{g2})	T_{mp}	T_m	ΔH_f/Jg^{-1} PBT
0 (PBT c.m.)	203.5	195.5	–	43.5	0.085	222.0	235.0	34.4
0(PBT, twin)	201.0	192.5	–	41.0	0.110	224.0	234.5	40.2
9.1 (c.m.)	204.0	196.5	−58.0	34.5	0.065	222.5	233.5	50.8
16.7 (c.m.)	206.5	195.5	−59.5	36.0	0.069	222.5	233.0	54.6
20 (twin scr)	201.5	195.0	−52.0	41.0	0.089	224.0	234.5	48.4
28.5 (c.m.)	203.0	195.5	−60.5	27.0	0.049	222.5	231.5	56.0
100.0 (liquid at RT)	–	–	65.0 ± 0.2 $\Delta Cp = 0.395$	–	–	–	–	–

The dimensions of the parameters in Table 3 are the following: T_{co}, T_{cp}, T_g, T_{mp}, T_m is °C; ΔC_p is Jg^{-1} g^{-1}; ΔH_f is Jg^{-1}; MAF and RAF are in %

Table 4 The phase structure of PBT/PN-250 blends

Sample	PBT T_g	MAF	α	RAF
PBT c.m	41	24	24	51
9.1% PN-250	37	20	39	41
16.7%PN-250	37	24	39	37
20% PN-250 (tw.scr)	22	32	35	33
28.5%PN-250	27	20	40	40

T_g, is in °C; MAF, α, RAF in %

increasing PN-250 content as expected (see Table 3). For the samples with 9.1, 16.7 and 28.5% PN-250 content, the T_g is −58.0, −59.5 and −60.5 °C, respectively.

Considering the data reported in Tables 3 and 4, and also in Fig. 11, it can be accepted that there is partial miscibility between PBT and PN-250. It is also clear that the PBT crystallinity in the blends is much higher than in neat PBT, and this could be the consequence of the higher mobility of PBT segments in the blends. It is also clear that the PBT crystallinity in the blends is much higher than in neat PBT, and this is the consequence of the higher mobility of PBT segments in the blends (Fig. 12).

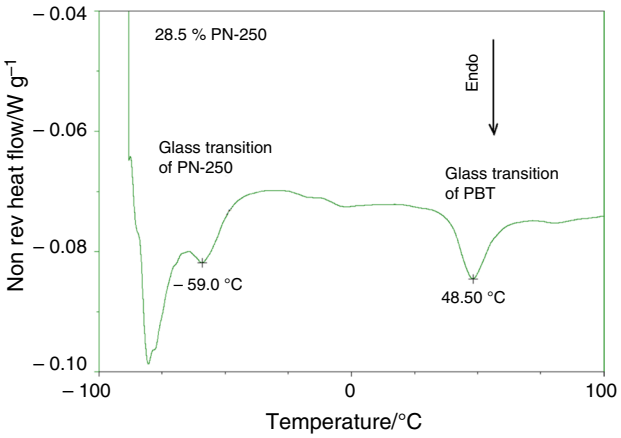

Fig. 11 The non-reversing heat flow as a function of temperature for a PBT/PN-250 blend with 28.5% of the plasticizer. The T_g of PN-250 is −59.5 °C, while the T_g of the PBT is 48.0 °C. Before the plasticizer's T_g the low temperature endotherm-like peak is the end of the isothermal → ramp mode change

Conclusions

1. The glass transition of many polymeric and low molecular mass samples can be determined by two methods:

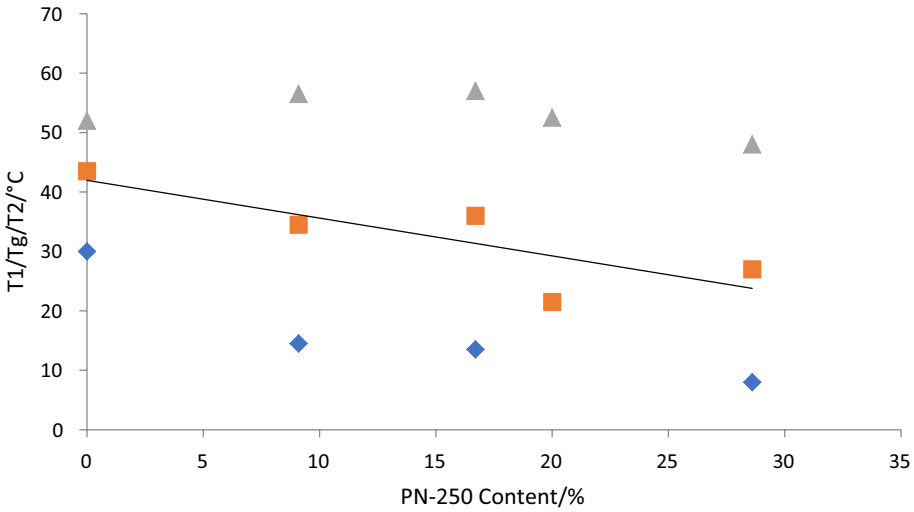

Fig. 12 The starting temperature of the glass transition (diamonds), the glass transition temperature (T_g, squares) and the end temperature of the glass transition (triangles) as a function of PN-250 content of the PBT-PN-250 blends as a function of PN-250 content. The straight line indicates the trend of the glass transition temperature with increasing PN-250 content

- In the first one, the approximate midpoint of the heat capacity jump of the glass transition can used,
- In the second method, a hysteresis peak can be created by slow cooling followed by fast reheating or annealing below the glass transition temperature, and the peak temperature in the Non-Reversing Heat Flow signal can be accepted as the glass transition temperature. The disadvantage of this method is that it does not allow determination of the heat capacity jump at the glass transition.

2. It is difficult to record the glass transition of PN-250, because it is close to the lowest temperature that can be achieved with an RC90 cooling unit of TA Instrument. This is complicated by the small PN-250 concentration in the PBT/PN-250 blends (sensitivity issues). Therefore, the hysteresis peak method needs to be used to determine the low temperature glass transition of the blends (the glass transition of the PN-250 rich areas).
3. PBT and PN-250 are partially miscible. The glass transitions of PN-250 and PBT move toward each other with changing composition.
4. The crystallization and melting properties of PBT are similar to those recorded for neat PBT.
5. The crystallinity of PBT in the blends is much higher than in neat PBT. This is due to higher segmental mobility in the blends.
6. The hysteresis peak at the PBT glass transition in the blends is much narrower and more intense than for neat PBT. This probably takes place because of the presence of higher and looser mobile amorphous fraction. Together with the lower rigid amorphous fraction this means that there is a sharper boundary between the mobile amorphous fraction and the PBT crystallites.
7. The developed hysteresis peak method seems to be a reliable method for determining the glass transition and its temperature when the low temperature baseline is missing.

References

1. Abraham T. Rubber compounding: chemistry and applications. Ch. 3. In: Rodgers B editor. New York: CRC Press; 2016.
2. Abraham T. Rubber compounding: chemistry and applications. Ch. 3. In: Rodgers B editor. New York: CRC Press; 2016:186
3. Abraham T. Rubber compounding: chemistry and applications. Ch. 3. In: Rodgers B editor. New York: CRC Press;2016:187
4. Abraham T. Rubber compounding: chemistry and applications. Ch. 3. In: Rodgers B editor. New York: CRC Press;2016:199
5. Kelly JR. Rubber & plastics news. Compounding of polyacrylate elastomers. 2013:14–19. Accessed 23 Sept 2013.
6. Ellul MD. Plasticization of polyolefin elastomers, semicrystalline plastics and blends crosslinked in situ during melt mixing. Rubber Chem Technol. 1998;71(2):244.
7. Qin J, Argon AS, Cohen RE. Toughening of glassy polymers by prepackaged deformation-activated diluents. J Appl Polym Sci. 1999;71:1469.
8. Argon AS. Craze plasticity in low molecular weight diluent-toughened polystyrene. J Appl Polym Sci. 1999;72:13.
9. Ehrenstein GW. Polymeric materials: structure-properties-applications. Hanser/Gardner Publications Inc.;2001.
10. Barton AFM. CRC handbook of solubility parameters and other cohesion parameters, 2nd ed. New York: CRC Press;1991.
11. Wang B, Shi B. Comparison of surface tension components and Hansen solubility parameters theories. Part I: Explanation of protein adsorption on polymers. J Macromol Sci B Phys. 2010;49:383.
12. Hansen C. The three dimensional solubility parameter and solvent diffusion coefficient and their importance in surface coating formulation. Copenhagen: Danish Technical Press;1967.
13. Hansen C. Hansen solubility parameters: a user's handbook. 2nd Ed. Boca Raton: CRC Press;2007. ISBN 978-0-8493-7248-3.
14. Fox TG. Influence of diluent and of copolymer composition on the glass temperature of a polymer system. Bull Am Phys Soc. 1956;1:123.

15. Gordon M, Taylor JS. Ideal copolymers and the second-order transitions of synthetic rubbers. I. Non-crystalline copolymers. J Appl Chem. 1952;2:495.
16. Menczel JD. To be published. 2023
17. Couchman PR, Karasz FE. A classical thermodynamic discussion of the effect of composition on glass-transition temperature. Macromolecules. 1978;11:117
18. Dechet A, Gómez Bonilla JS, Grünewald M, Popp K, Rudloff J, Lang M, Schmidt J. A novel, precipitated polybutylene terephthalate feedstock material for powder bed fusion of polymers (PBF): Material development and initial PBF processability. Materials & Design. Jan.2021;197:109265.
19. Cheng SZD, Pan R, Wunderlich B. Thermal Analysis of poly(butylene terephthalate) for heat capacity, rigid amorphous content, and transition behavior. Makromol Chem. 1988;188(10):2443.
20. Wunderlich B. Audio course in thermal analysis. Rensselaer Polytechnic Institute. 1980.
21. Menczel JD, Wunderlich B. Heat capacity hysteresis of semicrystalline macromolecular glasses. J Polym Sci Polym Lett Ed. 1981;19(5):261.
22. Menczel JD, Jaffe M. How did we find the rigid amorphous phase? J Therm Anal Calorim. 2007;89:357.
23. Oriol-Hemmerlin C, Pham QT. Poly 1, 3-butylene adipate Reoplex® as high molecular weight plasticizer for PVC-based cling films—microstructure and number-average molecular weight studied by 1H and 13C NMR. Polymer. 2000;41:4401.
24. Wunderlich B. Macromolecular Physics, Volume 3, Crystal Melting. New York, London, Toronto, Sydney, San Francisco: Academic Press;1980. ISBN 0-12-765603-0.
25. Menczel JD. Modulated thermal analysis techniques for characterizing the glass transition of semicrystalline polymers. In: 46th North American thermal analysis society meeting. Newport, RI. Accessed 5–8 Aug 2019.